



Water Spray Effects on Fire Smoke Stratification in a Symmetrical V-Shaped Tunnel

Jie Wang *, Dan Huang, Xiaowei Kong and Xuepeng Jiang, School of Resource and Environmental Engineering, Wuhan University of Science and Technology, Wuhan 430081 Hubei, China, Safety and Emergency Institute, Wuhan University of Science and Technology, Wuhan 430081 Hubei, China and Hubei Key Laboratory for Efficient Utilization and Agglomeration of Metallurgic Mineral Resources, Wuhan 430081 Hubei, China
Kaihua Lu, Faculty of Engineering, China University of Geosciences (Wuhan), Wuhan 430074 Hubei, China

Received: 11 December 2023/**Accepted:** 27 August 2024

Abstract. Smoke stratification in a V-shaped tunnel fire is complex due to the coupling effects of the double stack effect induced by the inclined tunnel structure, the fire thermal buoyancy, and the drag force caused by water spray system. This work investigates the influence of water spray flow rate (0 L/min to 600 L/min), atomization angle (0° to 150°) and distance between fire source and grade change point (0 m to 120 m) on smoke stratification in a symmetrical V-shaped tunnel through numerical simulations. The results show that the increase of water spray flow rate causes the increasing drag force which destabilizes smoke layer and contributes to the reduction of smoke layer thickness. While the water spray angle has little effect on smoke layer thickness. Through the dimensionless analysis and simulation results, a correlation for smoke layer thickness considering water spray parameters is proposed. Water spray effects on Fr describing the smoke stratification correspond to these on smoke layer thickness. That is, Fr decreases with the increase of water spray flow rate and is weak dependent on the water spray angle, and the critical Fr for turning point of the dominant effect of thermal buoyancy and drag force is linearly related to fire heat release rate. As the distance between fire source and grade change point increases, Fr changes a little on first double-slope control stage, increases on the left and decreases on the right of fire source, and eventually both levels off on second transition phase stage, thus tends to be stable on third single slope control stage.

Keywords: Tunnel Fire, Thermal stratification, Smoke stratification, Water spray flow rate, Water spray angle

List of Symbols

C_p Constant pressure specific heat capacity of air (kJ/(kg·K))
 D^* Diameter of combustion characteristics

* Correspondence should be addressed to: Jie Wang, E-mail: wangjie87@wust.edu.cn



F_d	Drag force induced by the water spray (N)
Fr	Source Froude number
g	Gravitational acceleration (m/s ²)
h	Smoke layer thickness (m)
h^*	Dimensionless smoke layer thickness
H	Tunnel height (m)
Δh	Smoke spreading height in the tunnel (m)
i	Tunnel slope (%)
l	Distance between fire source and V-shaped tunnel grade change point (m)
\dot{m}_w	Mass flow rate of the water spray (kg/s)
m_w	Total mass of water droplets in the interaction region with the smoke (kg)
P_f	Thermal buoyancy generated by density difference (N)
P_s	The driving force due to the double-slope stack effect (Pa)
q	Water spray flow rate (L/min)
q^*	Dimensionless water spray flow rate
\dot{Q}^*	Dimensionless fire heat release rate
\dot{Q}	Fire heat release rate (kW)
T_∞	Ambient air temperature (K)
$\square T_{max}$	Temperature rise (K)
T_a	Average smoke temperature through tunnel cross-section (oC)
u_a	Average flow velocity through tunnel cross-section (m/s)
$v_{z,in}$	Velocities of water droplets entering the smoke layer vertically (m/s)
$v_{z,out}$	Velocity of water droplets leaving the smoke layer vertically (m/s)
$V_{i,a}$	Smoke volume descending to the cool air layer (m ³)
$V_{i,s}$	Smoke volume directly acted upon by water droplets (m ³)
x	Distance from fire source (m)
θ	Water spray atomization angle (°)
ρ_∞	Air density (kg/m ³)
$\Delta\rho$	Density difference between smoke front and air (kg/m ³)
$\Delta\rho_{i,a}$	Density gap between smoke descending to the cool air layer and air (kg/m ³)
$\Delta\rho_{i,s}$	Density gap between the layer of smoke directly affected by water droplets and the layer of smoke without water droplets (kg/m ³)

1. Introduction

Underwater tunnels cross rivers, lakes or seas with a large gradient and height difference between the both sides and the middle part, and thus form a V-shaped structure. While underwater tunnels perform their functions, their fire characteristics are different from those of general tunnels due to their geographical location and V-shaped slope structure, which are mainly reflected in the fact that the traffic accident rate and the probability of fire in slope tunnels are much higher than those in horizontal tunnels [1–3]. In addition, under the influence of the chimney effect in inclined tunnels, the smoke will spread uphill [4], which makes it difficult to determine the direction of smoke movement and smoke control in V-tunnels. At the same time, the slope of the tunnel reduces the average escape velocity of personnel [5], which will increase the difficulty of emergency evacuation. Stable high smoke stratification can reduce the impact of fire smoke on the evacuation of trapped tunnel personnel [6]. The rapid cooling ability of water spray system is exactly suitable for tunnel fires, and water spray system has been adopted in many tunnels in China, such as the Wuhan Yangtze River Tunnel and the Xiamen Xiang'an Undersea Tunnel [7]. However, it can also disturb the stable smoke

layer to a certain extent, causing smoke settlement and endangering the safety of evacuees. Therefore, it is of great significance to study the effect of water spray system on smoke stratification in V-tunnel fires for effective fire smoke control and optimization of system parameters.

Due to geographical factors, existing tunnels are often not completely horizontal. When a fire breaks out in an inclined tunnel, the superimposed effect of the height difference between the exits at the two ends of the tunnel and the difference between the internal and external temperatures will produce a chimney effect, accelerating the diffusion and spread of high-temperature smoke uphill, and the movement of the smoke therefrom will be altered. Kang [8] also proposed that in the case of inclined tunnels with shafts for natural smoke evacuation, the smoke transport mechanism will be more complicated. Morlon [9] investigated both the thermal and the optical effects through the interaction of the water mist with the smoke layer produced by a fire, and concluded that, in order to provide the environmental complete characterization, both opacity measurements and temperature measurements should be made. Fan [10] used FDS to investigate the impact of roadway slope and length on smoke movement, and obtained a critical value of 100 for the number of Ri . Kong [11] proposes a non-dimensional empirical correlation of fire backing lengths for tilted tunnels with different slopes, where the dimensionless smoke backing lengths are logarithmically correlated with the cubic power of the downstream lengths. Cano-Moreno [12] proposes a quantitative method, based on linear multiple regression, that can account for the number of fatalities as a function of the delay in the start of evacuation and the slope of the tunnel, thus combining the consideration of the evacuation of tunnels as well as the effect of the slope of tunnels on the dispersion of gases and fumes. It should be noted that the above research work only focuses on single-slope tunnels, but the actual underwater tunnels often present multi-slope structures similar to the V, U, and W shapes due to the limitation of topography and other factors. These multi-slope tunnels have one or more variable slope points with up and down slopes, and the change of the relative positions of the fire source and the variable slope points will make the direction of thermal buoyancy complex, and its fire smoke transport characteristics are more special.

Some researchers have investigated water spray system effects on tunnel fire smoke control. Bullen [13] initially elucidated the impact of water mist on the stability of smoke stratification, attributing it to a delicate equilibrium between the resistance of water spray and the buoyancy of hot smoke. Bu [14] demonstrated that fine water spray controls smoke temperature and that the use of longitudinal ventilation significantly improves the fire stopping effect of water-spray fire suppression systems. Li [15] focused their research on studying the interaction between fine water spray and fire sources in tunnel configurations, utilizing both experimental and numerical methods. Luan [16] obtained that the smoke layer flow pattern may be disrupted by matching the sprinklers with the ventilation system. Wang [17] used simulations to examine the effects of water spray jet flow rate and spray angle on the critical velocity of longitudinal ventilation tunnels to obtain a unified correlation model for the critical velocity of such tunnels. Deng [18] suggest a hierarchical model of tunnel smoke and demonstrated that the cor-

relation between the drag effect of water spray and the size of droplets. Wang [19] used numerical simulation to introduce water spray intensity and momentum ratio to clarify the smoke barrier and thermal insulation effect. Obviously, the water spray will weaken the fire thermal buoyancy, change the mechanical ventilation, bilateral chimney effect, so that the smoke flow in multi-slope tunnels between the multiple driving forces of this and that produce a competitive relationship, resulting in the smoke flow in the bi-directional flow, transitional flow, unidirectional flow between the turning uncertainty; and the current research focuses on the influence of a single or two factors on the flow of the smoke, such as: natural and longitudinal ventilation under the single-slope tunnels, horizontal tunnels, etc., did not take into account the complexity of the coupling role of the water spray-multi-slope structure of the multifactor, and is also not in line with the actual application of the engineering situation.

A stable smoke layer during the expansion period of a one-dimensional plume can guarantee the safety of evacuation in case of fire, and is an important basis for the design of tunnel fire protection system parameters. Some researchers have investigated fire smoke stratification behavior and its stability criteria in a horizontal tunnel. For example, Newman [20] discovered an obvious smoke-air stratification related to a Froude (Fr) number especially under windless condition in ventilated duct fires, and divided fire smoke on fire source downstream into three regions according to Froude number values. Nyman and Ingason [21] conducted large-size experiments to verify the accuracy of Newman's smoke stratification Fr (<0.9), and found critical Fr 0.55. Ingason [22] found that thermal pressure and fire plume buoyancy contributed to stable smoke stratification and proposed the relationship correlation between thermal stratification and smoke concentration distribution. Huang [23] applied Newman's smoke stratification theory to a building corridor and proposed that smoke stratification is evident when Fr is less than 0.58. Tang [24] obtained that buoyancy stratification can be divided into stable stratification, stable stratification by some vortices, and unstable stratification where the upper buoyant smoke stream is strongly mixed with the lower stream. Li [25] explored the relationship between the height of the fire source and the hot smoke stratification upstream of the tunnel and found that the hot smoke stratification matched Newman's measurements regardless of the height of the fire source.

Most of the above domestic and international studies have been carried out in horizontal tunnels with water spray systems or slope tunnels without water spray systems, and have not yet dealt with the study of the influence of smoke layer characteristics under the combination of the two. When a fire occurs at different locations in a naturally ventilated underwater V-tunnel, the smoke is subject to the bilateral chimney effect and thermal buoyancy competing with each other to present three flow behaviors: bidirectional, transitional and unidirectional flow [26]. The V-slope of underwater tunnels is more complicated in smoke movement under the coupling effect of the two slopes, and the randomness of the position of the fire source also increases the uncertainty of the smoke movement, which, together with the cooling, dragging and blocking effects of the water spray, will make the smoke control more complicated. When a vehicle catches fire in a tunnel, its

location is difficult to be exactly at the point where the tunnel changes slope due to the uncertainty of the accident. When the location of the fire is not in the tunnel slope change point, because the location of the fire source and the tunnel exit on both sides of the elevation difference and density difference, both sides of the existence of the chimney effect, the fire smoke movement to produce competition, this time is called “double-slope stack effect”, high temperature and high toxicity of smoke spreading situation is more complex. In the event of a fire, the uphill section of a V-slope tunnel becomes the main channel for the rise of hot air and smoke. Due to the change in gradient, hot air rises more rapidly in the uphill section, creating a pronounced chimney effect. Concurrently, cold air from the downhill section or the tunnel entrance is drawn into the tunnel due to the lower pressure in the uphill section, supplementing the heated and rising air. In single-slope tunnels, smoke typically spreads uphill, with the chimney effect being directly proportional to the slope; that is, a larger slope results in a more pronounced chimney effect. In a fully symmetrical V-slope tunnel, where the slopes are reversed, smoke may exhibit different spreading patterns on either side, potentially competing against or offsetting the chimney effect.

Therefore, this paper comprehensively analyzes the effects of the symmetrical V-shaped double slope gradient, water spray flow rate and angle on the maintenance of stable fire smoke stratification when the water spray system is employed. The aim is to determine the stability law of tunnel smoke stratification and put forward the theoretical support for the prevention and control of smoke in the tunnel.

2. Theoretical Analysis

2.1. Smoke Stratification Mechanism

The purpose of this study was to better understand the smoke deposition phenomena that may occur in a fully symmetrical V-slope tunnel fire using water spray system. Smoke thermal stratification refers to the phenomenon where the fire approximates the tunnel into two distinct layers: the upper part, which is high-temperature smoke, and the lower part, which is cold air. High-temperature smoke exhibits stratification due to the combined effects of thermal buoyancy and horizontal inertia forces during a fire [27, 28]. To effectively control smoke, the water spray system must be activated promptly. The sprayed water droplets can disrupt the relatively stable smoke layer, potentially leading to significant smoke settling. Previous studies [13, 29, 30] have identified two fundamental mechanisms by which water droplets induce smoke settling: the downward drag force exerted on the surrounding gas, and the cooling effect that reduces the buoyancy of the smoke.

Within the direct-action area of the water spray system (i.e., within 30 m of the fire source), the smoke is subjected to a drag force from the water spray system. Additionally, the lower temperature of the water droplets compared to the smoke leads to heat exchange, which reduces the smoke’s temperature and, by the principles of ideal gas behavior, increases its density. In areas not directly affected by

the water spray, the interaction between the water and smoke is minimal. This results in the high-density smoke in these regions experiencing downward buoyancy relative to the lower-density smoke in the surrounding environment. As the smoke settles under the dual influence of the water spray's drag force and its own downward buoyancy, the settled smoke, despite having increased in density due to cooling by water droplets, remains lighter than the lower layer of cold air. Consequently, the smoke will begin to exhibit upward buoyancy. As the settling smoke accumulates and its volume increases, the upward buoyancy also increases. Once the upward buoyancy balances the downward forces, the smoke will cease to settle and stabilize at a certain height. Tang [31] proposed a new combined force equilibrium system considering the downward drag force exerted by the water particles on the surrounding gas and the cooling effect of the water particles on the smoke resulting in the reduction of the smoke buoyancy. In conjunction with this paper, taking the double slope stack effect induced by the V-shaped tunnel structure into consideration, a new driving force balance relationship (the drag force of the water spray F_d , the stack effect of left tunnel $P_{s,l}$, the stack effect of right tunnel $P_{s,r}$, and the thermal buoyancy P_f) for fire smoke in a V-shaped tunnel is given in Fig. 1.

$$F_d = \dot{m}_w(v_{z,in} - v_{z,out}) + m_w g \cos i \tag{1}$$

where \dot{m}_w and m_w are the mass flow rate and the total water particle mass interacting with fire smoke respectively, kg/s and kg; $v_{z,in}$ and $v_{z,out}$ are the vertical velocities of water droplets entering and leaving the smoke layer respectively, m/s; i is the inclination angle of the tunnel.

P_A is the buoyancy of the smoke in the region where the water droplets interact with the original smoke layer, N; P_B is the buoyancy in the region of the smoke that descending to the lower layer of cold air, N. So a total thermal buoyancy can be expressed [32] by

$$P_f = P_A - P_B = (\Delta\rho_{i,a}V_{i,a} - \Delta\rho_{i,s}V_{i,s})g \cos i \tag{2}$$

where $\Delta\rho_{i,a}$ and is the density difference between smoke settling into the cool air layer air and the cool air, kg/m³; $V_{i,a}$ is the settling smoke volume into the cool air layer, m³; $\Delta\rho_{i,s}$ is the density difference between the smoke layer interacting with water droplets and that without water droplets, kg/m³; $V_{i,s}$ is the smoke volume interacting water droplets, m³.The total driving force caused by the double slope stack effect of left and right tunnel part is:

$$P_s = \Delta\rho\Delta h g \cos i \tag{3}$$

where $\Delta\rho$ is the density difference between smoke front and air, kg/m³; Δh is the smoke spreading height, m.

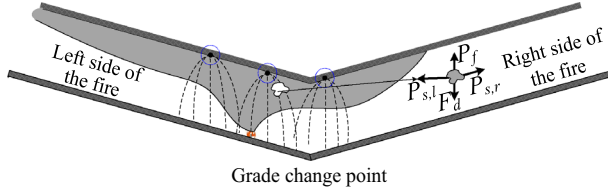


Figure 1. Driving forces for fire smoke in a V-shaped tunnel.

2.2. Dimensionless Analysis

In tunnel, the smoke layer thickness is related to the following factors: fire heat release rate Q , tunnel height H , symmetrical V-shaped tunnel gradient i , ambient air temperature T_∞ , ambient air density ρ_∞ , constant pressure specific heat capacity of air c_p , gravitational acceleration g , and water spray flow rate q . Then the following relationships can be listed:

$$f(Q, h, H, i, T_\infty, \rho_\infty, C_p, g, q) = 0 \quad (4)$$

According to the π -theorem, H , ρ_∞ , T_∞ , and g as the basic parameters, a new expression for Eq. (4) is given:

$$f(\pi_1, \pi_2, \pi_3, \pi_4, \pi_5) = 0 \quad (5a)$$

where

$$\begin{cases} \pi_1 = H^{\alpha_1} \rho_\infty^{\beta_1} T_\infty^{\gamma_1} g^{\delta_1} h \\ \pi_2 = H^{\alpha_2} \rho_\infty^{\beta_2} T_\infty^{\gamma_2} g^{\delta_2} Q \\ \pi_3 = H^{\alpha_3} \rho_\infty^{\beta_3} T_\infty^{\gamma_3} g^{\delta_3} i \\ \pi_4 = H^{\alpha_4} \rho_\infty^{\beta_4} T_\infty^{\gamma_4} g^{\delta_4} C_p \\ \pi_5 = H^{\alpha_5} \rho_\infty^{\beta_5} T_\infty^{\gamma_5} g^{\delta_5} q \end{cases} \quad (5b)$$

The following 5 dimensionless terms are obtained through dimensional analysis:

$$\begin{cases} \pi_1 = h/H \\ \pi_2 = Q/(\rho_\infty g^{3/2} H^{7/2}) \\ \pi_3 = i \\ \pi_4 = T_\infty C_p/(gH) \\ \pi_5 = q/(H^{5/2} g^{1/2}) \end{cases} \quad (6)$$

Expressing Eq. (5) can be achieved by the following equation:

$$f\left(\frac{h}{H}, \frac{Q}{\rho_\infty g^{3/2} H^{7/2}}, i, \frac{T_\infty C_p}{gH}, \frac{q}{H^{5/2} g^{1/2}}\right) = 0 \quad (7)$$

By the similarity principle, Eq. (7) can be converted to:

$$\frac{h}{H} = f\left(\frac{Q}{\rho_{\infty} g^{3/2} H^{7/2}}, i, \frac{T_{\infty} C_p}{gH}, \frac{q}{H^{5/2} g^{1/2}}\right) \quad (8)$$

Equation (8) is also expressed as:

$$h^* = f(Q^*, i, q^*) \quad (9)$$

where $h^* = \frac{h}{H}$, $Q^* = \frac{Q}{\rho_{\infty} T_{\infty} C_p g^{1/2} H^{5/2}}$, $q^* = \frac{q}{g^{1/2} H^{5/2}}$.

Calculations show that the tunnel gradient i , dimensionless fire heat release rate Q^* , and dimensionless water spray system flow rate q^* are the factors influencing the dimensionless smoke layer thickness in a symmetrical V-shaped tunnel.

2.3. Froude Number for Smoke Stratification

Smoke stratification criteria Fr is related with the smoke temperature stratification and can be calculated by [21]:

$$Fr = \frac{u_{avg}}{\sqrt{\frac{\Delta T_{cf}}{T_{avg}} Hg}} \quad (10)$$

where, u_{avg} and T_{avg} represent the average flow velocity and average smoke temperature of the tunnel cross-section, respectively; ΔT_{cf} is the smoke temperature difference between beneath ceiling ($0.88H$) and under floor ($0.12H$), °C; H is the tunnel height, m; take $g = 9.81 \text{ m/s}^2$.

For a given tunnel, Fr is determined by the smoke flow rate and temperature which can be changed by water spray system directly. Therefore, Fr values for smoke stratification would be different from those without water spray system.

3. Numerical Methods

3.1. Fire Scenarios

In this paper, fire simulation calculations using Fire Dynamics Simulator (FDS) version 6.6.0 have been carried out to investigate fire scenarios in tunnels with natural ventilation systems. Smoke layer height is an important indicator of the safety of people in the flow of smoke from a road tunnel fire. In FDS, the smoke layer height is predicted and calculated using the method proposed by Janssens [33]. based on the cross-sectional vertical smoke temperature distribution, which has been widely used in previous studies [34–36]. In this method, the temperature T_z is considered to be a continuous function between the floor ($z = 0$) and ($z = H$) the ceiling with respect to the height z . T_{low} is assumed to be a constant equal to the value of the temperature of the cell closest to the floor, and T_{up} varies as a vertical gradient with height. The formulae for these two temperatures are given below:

$$(H - h)T_{up} + hT_{low} = \int_0^H T(z)dz = I_1 \quad (11)$$

$$(H - h)\frac{1}{T_{up}} + h\frac{1}{T_{low}} = \int_0^H \frac{1}{T(z)} dz = I_2 \quad (12)$$

$$h = \frac{T_{low}(I_1 I_2 - H^2)}{I_1 + I_2 T_{low}^2 - 2T_{low}H} \quad (13)$$

where T_{up} is the upper layer temperature, K; T_{low} is the lower layer temperature, K; H is the ceiling height, m; and h is the smoke layer interface height, m.

FDS can simulate and solve all kinds of fire scenarios flexibly by using the above set of equations, and can predict the changes and flow patterns of smoke temperature, co and other substances during the dynamic development of fire. More information on the theory and algorithms of the numerical simulation method and validation can be found in the FDS User Guide [37].

As shown in Fig. 2(a), the tunnel foundation model, built by FDS [38], measures 600 m in length, 13.2 m in width, and 8.1 m in height. Based on this model, three different scenarios with tunnel gradients of 0%, 3%, and 5% are studied. The fire source in the simulation uses n-heptane as fuel, with dimensions of 4.5 m 3 m 2 m, and the fire type is set as a constant fire source. The rate of heat release is set to 5 MW, 10 MW, 15 MW, and 20 MW, respectively, and does not change with time. The two ends of the tunnel are defined as ‘OPEN’, and the boundaries of the roof, side walls, and floor of the tunnel are defined as ‘CONCRETE’. The thermophysical properties are based on those of actual concrete materials [39, 40]. The specific heat is 1.04 kJ/(kg·K), the density is 2280 kg/m³, and the thermal conductivity is 1.8 W/(m·K). The entire tunnel is naturally ventilated, with an ambient temperature of 20 °C.

According to the results of previous studies, the vertical location of the maximum temperature in the tunnel is 0.02H below the roof, where H is the tunnel height [41]. Therefore, a series of temperature measurement points were arranged along the longitudinal center line of the tunnel at 0.16 m below the roof, with a distance of 1.5 m. Vertical temperature and velocity measurement points were set up from 3 m away from the fire source, with a spacing of 0.2 m. The temperature and velocity measurement points were set up at 0.2 m apart, with a spacing of 1.5 m from the fire source. Water spray nozzles were installed at a distance of 5 m on both walls at a height of 4.5 m. The flow rate and angle of the water jets were adjustable from 0 L/min to 250 L/min and from 0° to 150°, respectively.

Considering that fires can occur at various locations within the tunnel, the distance of the fire source from the slope change point is defined as the ‘fire source location’. This distance is specified at 0 m, 10 m, 20 m, 40 m, 60 m, 80 m, 100 m, and 120 m. The fire source is uniformly positioned along the left side of the tunnel at these locations. In total, there are 315 groups of working conditions, with

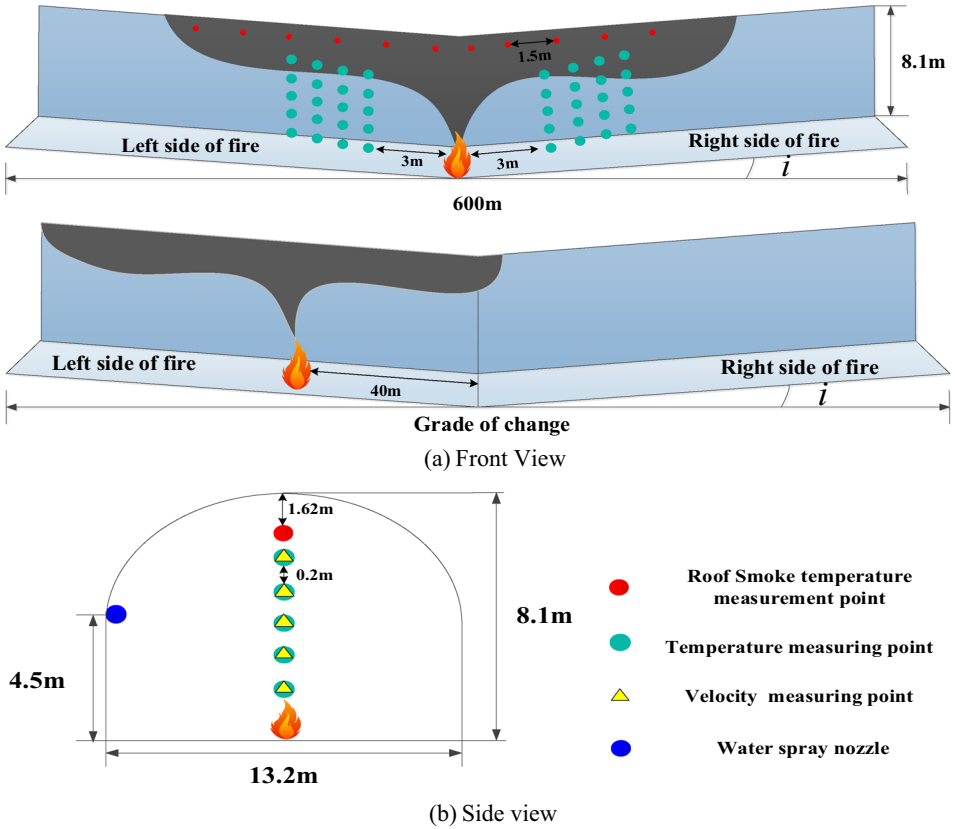


Figure 2. V-shaped slope tunnel fire simulation schematic.

detailed parameters provided in Table 1. The output data, including smoke temperature and visibility, reach a stable state at about 300 s. Therefore, the analysis presented below utilizes the mean values of the output data recorded between 300 s and 400 s.

3.2. Grid Independence Analysis

FDS user guide recommends to adopt the grid size from $1/16D^*$ to $1/4D^*$ [37], where the fire characteristic diameter D^* is defined by:

$$D^* = \left(\frac{Q}{\rho_\infty c_p T_\infty \sqrt{g}} \right)^{2/5} \quad (14)$$

where Q is fire heat release rate, kW; ρ_∞ is ambient air density, 1.02 kg/m^3 ; c_p is air constant pressure specific heat capacity, $1.004 \text{ J/(kg}\cdot\text{K)}$; T_∞ is the ambient air temperature, 293.15 K ; g is gravity acceleration, 9.81 m/s^2 . From Eq. (14) it can

Table 1
Tunnel Model Working Condition Table

Serial number	Water spray flow (L/min)	Water spray atomization Angle (°)	Distance of fire source from gradient point (m)	HRR (MW)	Tunnel slope
1 to 105	0, 10, 50, 100, 200, 400, 600	120	0	5, 10, 15, 20, 25	0%, 3%, 5%
106 to 195	250	0, 30, 60, 90, 120, 150	0		
196 to 315	250	120	0, 10, 20, 40, 60, 80, 100, 120		

be seen that for fire heat release rates of 5 MW to 25 MW, grid sizes are calculated from 0.15 m to 0.60 m.

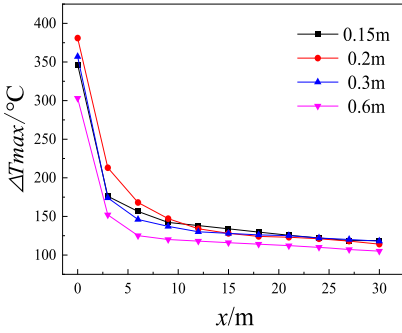
Four grid sizes, 0.15 m, 0.20 m, 0.30 m and 0.60 m, were selected to verify their accuracy by comparing the maximum smoke temperatures along the length of the tunnel without and with water spray in Fig. 3(a, b). The variation curves of the smoke and its temperature for the grid size of 0.3 m is basically the same as those for the grid sizes of 0.15 m and 0.2 m were found to be the same. Many studies [42, 43] have shown that the FDS model can be validated based on the differences in maximum smoke temperatures at different locations. Meanwhile, the construction of Li [44] model mainly relies on the size and magnitude analysis, which is exactly the same in this paper. The Li model is simulated in this paper without longitudinal ventilation at velocity less than 0.19, and the numerical comparison of the simulation is shown in Fig. 3, the simulated tunnel roof smoke temperature at 0.3 m grid size is consistent with the experimental results of Li. Therefore, a 0.3 m grid is chosen in this paper.

4. Results and Discussion

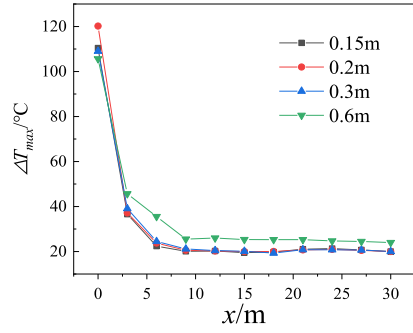
4.1. Water Spray Flow Rate Effect on Smoke Stratification

When a fire occurs in the tunnel, fire smoke driven by thermal buoyancy flows vertically, continuously impinges the tunnel ceiling into horizontal flow, and then turns into a one-dimensional longitudinal flow due to the sidewall restriction [33]. The average smoke layer thickness values between 10 m to 30 m from fire source in water spray zone are analyzed here [45].

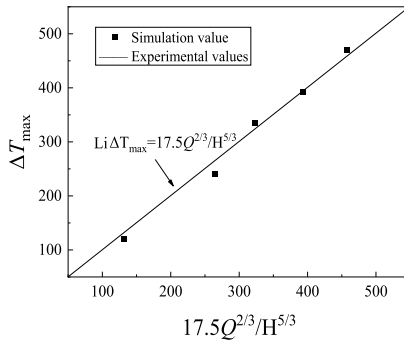
Figure 4. shows the smoke layer thickness changes with increasing water spray flow rates in the V-shaped tunnel with different slopes. Overall, the smoke layer thickness decreases with the increase of the water spray flow rate. In the case of the same tunnel gradient and the same water spray flow rate, the fire heat release rate is high, the amount of fire smoke produced is large, and the smoke layer thickness becomes thicker accordingly. In the case of the same fire heat release rate and the same water spray flow rate, the smoke layer thickness tends to



(a) Variation of maximum smoke temperature along the length of the tunnel for different grid sizes without water spraying



(b) Variation of maximum smoke temperature along the length of the tunnel for different grid sizes with water spraying



(c) Comparison of maximum temperature simulation values with previous values

Figure 3. Grid independence and simulation accuracy analysis.

decrease with the increase of the tunnel gradient. This is due to the slope of the tunnel stack effect is more obvious, the tunnel smoke force is greater, so that the thin smoke layer below the stable smoke further upward cohesion. And in the case of the same tunnel slope, the same fire heat release rate, high water spray flow rate than low water spray flow rate smoke layer thickness is smaller. That is, it indicates that more toxic smoke settles into the air layer, thus affecting the evacuation of people in the tunnel.

Since the smoke layer thickness is proportionate to smoke yield which is a power function relationship with fire heat release rate based on classical fire plume mass flow rate model [31], Eq. (15) can be given as:

$$\frac{h^*}{Q^{*0.33}} = f(i, q^*) \tag{15}$$

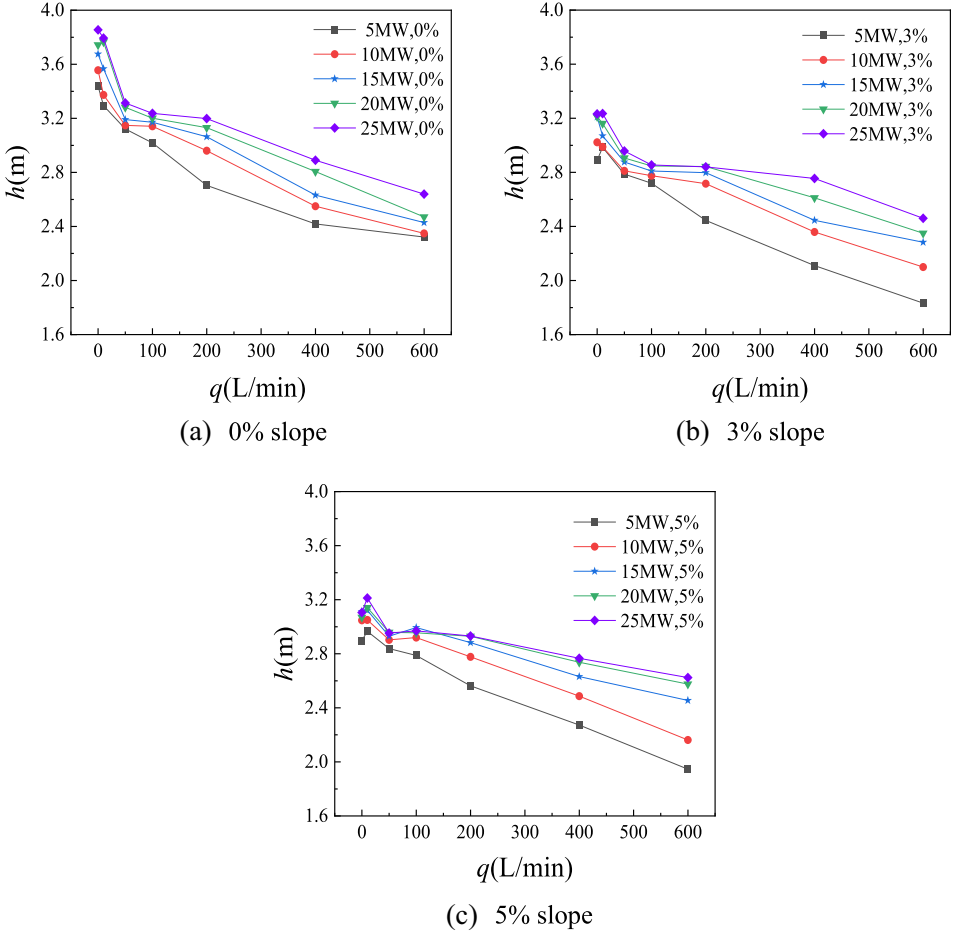


Figure 4. Variation curve of smoke layer thickness with water spray flow in the V-shaped tunnel with different slopes.

According to simulation data and Eq. (15), The dimensionless smoke layer thickness in the symmetric V-shaped tunnel is illustrated in Fig. 5 as follows:

$$h^* = [(2.50i - 0.35)q^* + (-2.69i + 1.08)]Q^{*0.33} \quad (16)$$

Figure 6 plots average Fr values for smoke flow within 10 m to 30 m from fire source in the V-shaped tunnel fires with different fire heat release rates and slopes versus normalization water spray flow rate. Obviously, Fr initially decreases and then steadily increases as the water spray flow rate increases. When the water spray flow rate is less than 50 L/min ($q^* = 0.6$), its effect on the thermal buoyancy force P_f and drag force F_d is weak. And because $P_f > F_d$, that is, the upward driving force is stronger than the downward driving force, smoke gathers beneath the

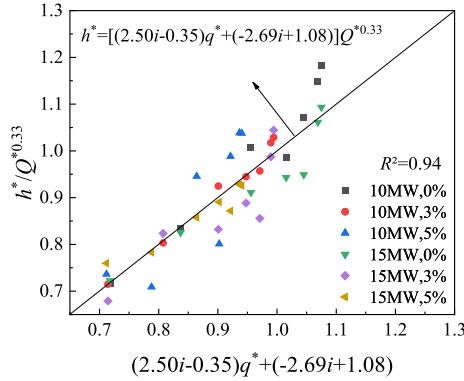


Figure 5. Correlation for smoke layer thickness in the V-slope tunnel considering water spray flow rate effect.

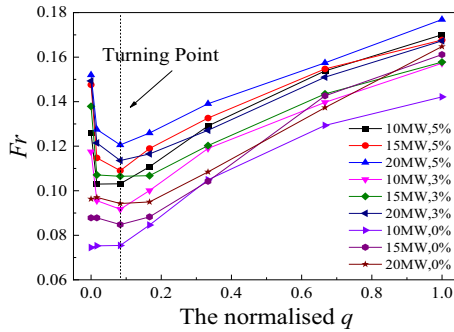


Figure 6. Fr for smoke stratification in the V-shaped tunnel fires with different fire heat release rates and slopes versus normalization water spray flow rate.

ceiling and settles little. At these conditions, Fr gradually decreases as the water spray flow rate increases, and the smoke layer thickness changes little. After the water spray flow rate increases to 50 L/min ($q^* = 0.6$), P_f decreases and F_d increases because of the stronger cooling effect. Overall $P_f < F_d$, that is, the upward driving force is weaker than the downward driving force, the temperature of the tunnel ceiling decreases, and the fire smoke gradually sinks. At this time, Fr increases with the increase of spray flow, and the smoke layer thickness gradually decreases.

Regarding this one, the tendency for the Fr number to show a decreasing and then increasing trend with increasing flow in horizontal tunnels is relatively less pronounced. It is because the increase in tunnel slope enhances the stack effect force P_s , so fire smoke flows faster. From Sect. 2.3, Fr is proportional to the aver-

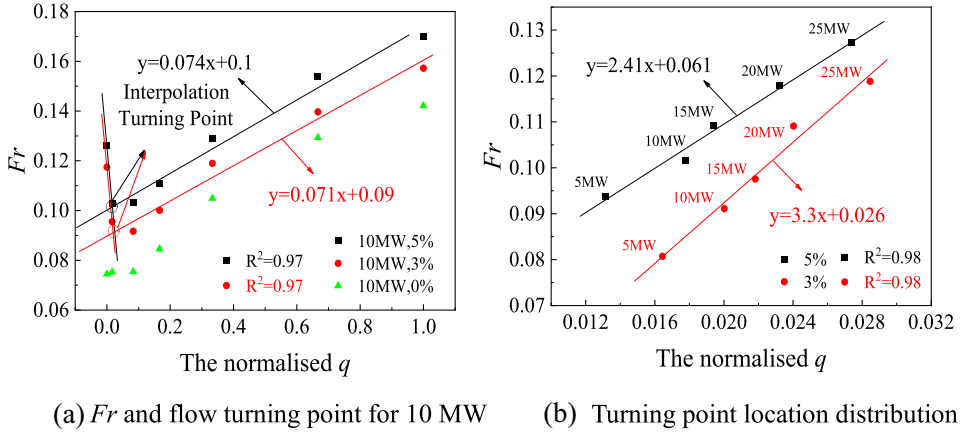


Figure 7. Fr and critical Fr values for V-shaped tunnel fires of different heat release rates and water spray flow rates.

age smoke flow velocity through tunnel cross-section, so corresponding Fr is larger in larger sloped tunnel in Fig. 6.

To investigate the turning point of Fr with the increase of water spray flow rate, a fitted straight line of the falling and rising segments of Fr values for 10 MW tunnel fires is plotted in Fig. 7(a). When Fr is less than turning point, smoke flow is dominated by P_f . While Fr is larger than turning point, the dominated factor of smoke flow changes into F_d . Figure 7(b) gives Fr values at turning points (Critical Fr) for all V-shaped tunnel fires of various heat release rates and slopes. Clearly, critical Fr increases as fire heat release rate increases, and Fr 's corresponding water spray flow rate increases. Because larger fire heat release rate enhances smoke temperature and flow rate and leads to smoke settling at a larger water spray flow rate. Critical Fr values for 5% sloped tunnel is larger than those for 3% now in Fig. 7(b). Critical Fr line for 3% sloped tunnel would intersect with that for 5%, when heat release rate increases continuously, indicating that the stack effect on smoke stratification is outplayed by thermal buoyancy effect of higher fire heat release rate.

4.2. Water Spray Angle Effect on Smoke Stratification

Figure 8 shows the smoke distribution of 10 MW 3% slope tunnel fires with various angles from $0^\circ \sim 150^\circ$ of the water spray system. For tunnel fires without water spray system, the fire smoke appears as one-dimensional longitudinal flow within the middle zone of the V-shaped tunnel right and left side. Smoke flow stratification in the tunnel can be approximately classified into three layers including the upper layer with high-temperature smoke, the middle layer with smoke-air mixing and the lower layer with cold air as shown in Fig. 9(a). After the activation of the

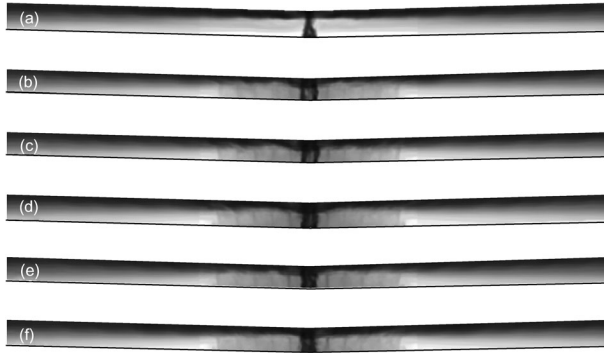


Figure 8. Smoke distribution of 3% sloped tunnel fires with 10 MW under different water spray angles (a) 0°, (b) 30°, (c) 60°, (d) 90°, (e) 120°, f 150°.

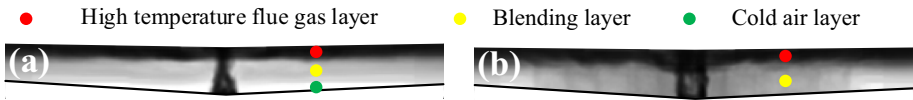
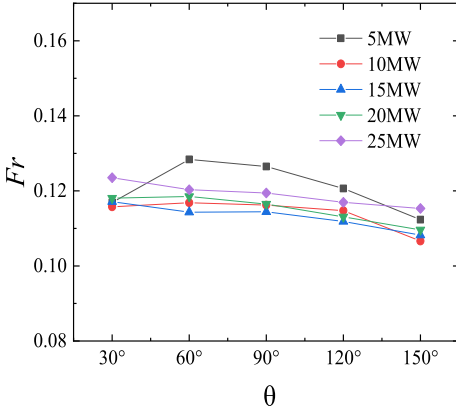


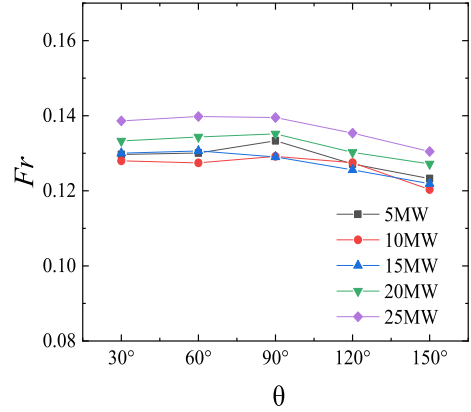
Figure 9. Schematic diagram of smoke stratification in the V-shaped tunnel: (a) without water spray, (b) with water spray.

water spray system, fire smoke moves downward gradually under the action of drag force F_d , and blends with the cold air to form smoke-air mixing layer. The original three layers in the tunnel without water spray are disturbed by the water spray system, and the cold air layer gradually disappears. Finally there are only the upper high-temperature smoke layer and lower smoke-air mixing layer as shown in Fig. 9(b). By comparing smoke distribution in Fig. 8, it is not intuitively apparent that the increase of water spray angle has obvious influence on fire smoke spread process.

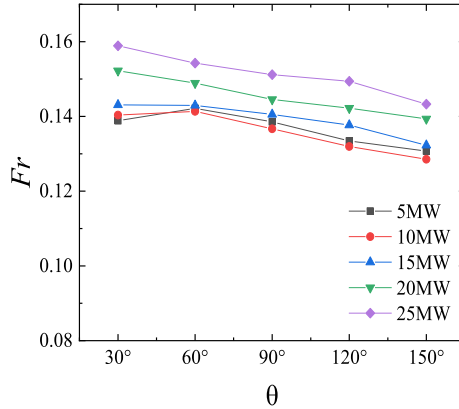
Figure 10 plots Fr values for V-shaped tunnel fires of different heat release rates and water spray flow rates, which fluctuates little and have a little bit of a downward trend as water spray angle increases in sloped tunnels. Because the action area of water spray droplets on smoke is enhanced, the drag force F_d on the same volume smoke becomes less. And then the smoke subsidence degree is reduced, thus forming more stable smoke layer. Fr values in 0%, 3%, 5% slope tunnel fluctuate within 0.007, 0.009, 0.011 respectively, and the overall fluctuation is basically within 5%. Therefore, in the V-shaped tunnel fires, the effect of water spray angle on Fr is very small, which is basically the same as its effect on smoke layer thickness in Sect. 4.1, that is, the angle of water spray system in a V-shaped tunnel has little effect on Fr .



(a) 0% slope



(b) 3% slope



(c) 5% slope

Figure 10. Fr values for V-shaped tunnel fires of different heat release rates and water spray angles.

4.3. Fire Source Location Effect on Smoke Stratification

In this paper, when considering the increase in the distance between the fire source and the variable slope point of the tunnel, the influence on the smoke layer thickness of the tunnel is divided into three phases: (I) double-slope control phase, where the distance between the fire source and the variable slope point of the tunnel is 0 m to 10 m; (II) transition phase, where the distance between the fire source and the variable slope point of the tunnel is 20 m to 80 m; and (III) single-slope control phase, where the distance between the fire source and the variable slope point of the tunnel is 100 m to 120 m. The fire source and the variable slope point of the tunnel are divided into three phases.

Figure 11 depicts smoke spread in 10 MW V-shaped tunnel fires at various slopes, with the fire source located 120 m away from the grade change point (fire source moves to the left from the centre at 0% gradient). Obviously, fire smoke in 0% slope tunnel spreads to the right tunnel opening, and that in 3% slope tunnel

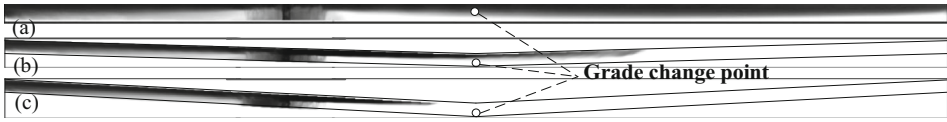


Figure 11. Smoke spread of 10 MW V-shaped tunnel fires when fire source is 120 m from the grade change point (a) 0% slope, (b) 3% slope, (c) 5% slope.

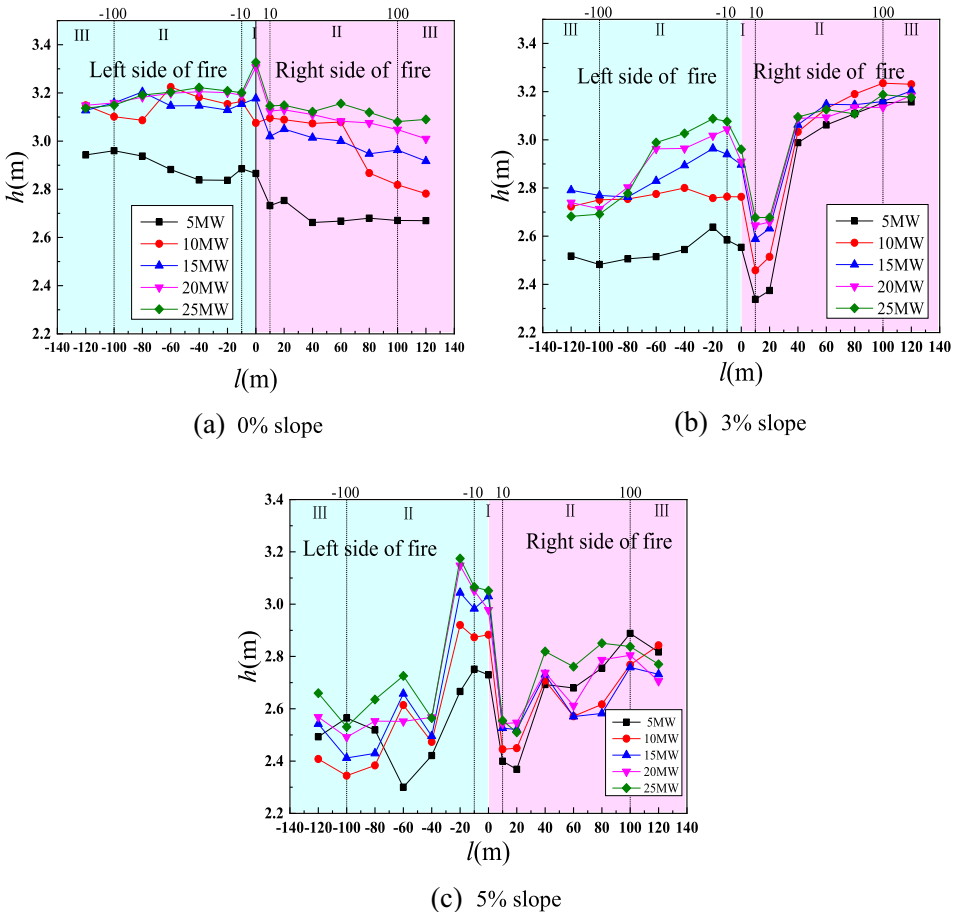


Figure 12. Smoke layer thickness of V-shaped tunnel fires sources with different heat release rates and slopes versus the distance between fire source and grade change point.

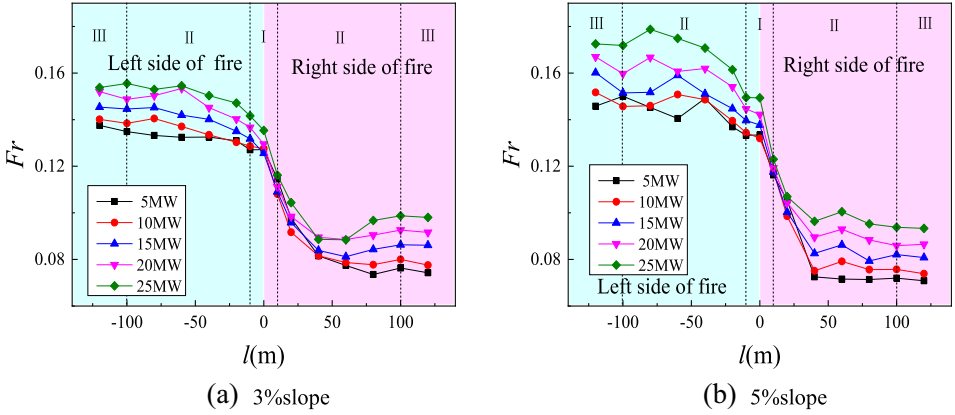


Figure 13. Fr curve of the distance of fire source from the variable slope point in tunnels with different slopes.

Table 2
Average Fr Values on the Third Stage (Single-Slope Control Stage)

HRR(MW)	3% slope		5% slope	
	Left side of fire	Right side of fire	Left side of fire	Right side of fire
5	0.135	0.076	0.150	0.072
10	0.138	0.080	0.146	0.076
15	0.145	0.086	0.151	0.082
20	0.149	0.093	0.160	0.086
25	0.156	0.099	0.172	0.094

spreads to the middle zone of the right tunnel, while fire smoke in 5% slope tunnel still does not spread to the grade change point. In other words, fire smoke spreads downstream slower from fire source location to the grade change point, as the tunnel slope increases. Because the coupling right and left stack effect force P_s increases in a large slope tunnel, blocks smoke spreading to the grade change point.

To examine how the distance between the fire source and grade change point affects the smoke layer thickness, Fig. 12 plots smoke layer thickness in V-shaped tunnel fires with various heat release rates and tunnel slopes. The three regions, labeled as I, II, and III, represent different stages: the double-slope control stage, the transition stage, and the single-slope control stage, respectively [26]. Different from the temperature change in previous study, on the double-slope control stage, there is considerable difference of the smoke layer thickness between the left and right of fire source. Because a large amount of smoke gathers between tunnel grade change point and fire source location, when fire source moves 10 m to the left of the tunnel grade change point, the smoke layer thickness on the tunnel right side decreases. on the single slope control stage, the smoke layer thickness changes less and basically stabilize.

Figure 13 shows Fr values of 3%, 5% V-shaped tunnel fires with different heat release rates versus the distances from fire source to grade change point. On the double-slope control stage, Fr changes a little, which is consistent with the smoke layer thickness trend. On transition phase, Fr increases on the left and decrease on the right of fire source, and eventually both levels off. On the single slope control stage, Fr for the same heat release rate tends to be stable, when the distance from fire source location to the tunnel grade change point increase. The average Fr values are summarized in Table 2.

5. Conclusions

The influence of water spray system parameters (flow rate and angle) and fire source location on smoke spread in V-shaped tunnel fires are investigated through theoretical and numerical simulation analysis. The smoke layer thickness and Fr values are obtained to explain the change law. The conclusions include as follows:

An increase in water spray flow rate causes a decrease of the smoke layer thickness. A correlation for smoke layer thickness considering the flow rate of water spray system and tunnel slope is proposed through the dimensionless analysis and simulation data analysis. Correspondingly, Fr shows an increasing and then decreasing trend with the increase of the flow rate of the sprinkler system, and the critical Fr at the turning point of the dominant effect of thermal buoyancy and drag is linearly related to the rate of fire-heat release. However, the influence of fire-heat release rate on Fr can gradually exceed the superposition effect of V-tunnel.

- 1) Decreases with the increasing flow rate of water spray system, and the critical Fr for turning point of the dominant effect of thermal buoyancy and drag force is linearly related to fire heat release rate. The effect of fire heat release rate on Fr can gradually overtake the stack effect of V-shaped tunnels.
- 2) Water spray system flow rate is certain, the atomization angle increases, the smoke layer thickness decreases, the Fr number becomes smaller, but the fluctuations are small. The water spray flow with a large atomization angle reduces the smoke temperature and attenuates the radiant heat feedback, which can indirectly inhibit the combustion reaction. Therefore, when the water flow rate is certain, increasing the atomization angle is conducive to reducing the concentration of smoke in the downwind direction of the fire source, and the phenomenon of smoke layer settling and turbulence is relatively light.
- 3) Smoke spread in a V-shaped tunnel can be divided into three stages on the basis of the change of dominant driving force, as the distance between the tunnel grade change point and fire source location increases. Due to coupling effects of double-slope stack effects, thermal buoyancy and drag force induced by water spray system, Fr changes a little on first double-slope control stage, increases on the left and decreases on the right of fire source, and eventually both levels off on second transition phase stage, thus tends to be stable on third single slope control stage.

Acknowledgements

This study was supported by the National Natural Science Foundation of China under Grant No. 52476127 and 52376133.

Funding

National Natural Science Foundation of China, 52476127, Jie Wang, 52376133, Kaihua Lu.

References

1. PIARC Committee on Road Tunnels (C5) (1999) Fire and smoke control in road tunnels. PIARC Committee on Road Tunnels, Paris
2. Wei W (2000) Traffic engineering. Southeast University Press, Nanjing, pp. 219–220 in Chinese
3. Economic and Social Council (2001) Recommendations of the group of experts on safety in road tunnel. Economic and Social Council, New York
4. Peng JZ (2011) Study on the influence of slope on smoke spreading characteristics of extra-long highway tunnel fire. Central South University, D Changshain Chinese
5. Tang XF (2017) An experimental study of the effect of slope on evacuation. *J Fire Sci Technol* 11:1508–1511(in Chinese)
6. Yang LL, Fan CG, Luan D, Ouyang RC, Tao HW, Xu ZS, Wang FY (2021) Experimental study on thermal stratification characteristics in tunnel fires under the effect of canyon cross wind. *J Wind Eng Ind Aerod* 218:104756. <https://doi.org/10.1016/j.jweia.2021.104756>
7. Tang Z, Fang Z (2016) Study of the effect of tunnel sprinkler systems on critical wind speeds. *J Fire Sci Technol* 35(2):224–227(in Chinese)
8. Li Q, Kang JH, Wu YT, Luo J (2022) Theoretical and numerical study of smoke back-layering length for an Inclined tunnel under longitudinal ventilation. *Fire Technol* 58(4):2143–2166. <https://doi.org/10.1007/s10694-022-01250-1>
9. Morlon R, Boulet P, Parent G et al (2015) Study of de-stratification and optical effects observed during smoke/mist interactions. *Fire Technol* 51:1231–1248. <https://doi.org/10.1007/s10694-014-0437-y>
10. Fan CG, Li XY, Mu Y, Guo FY, Ji J (2017) Smoke movement characteristics under stack effect in a mine laneway fire. *Appl Therm Eng* 110:70–79. <https://doi.org/10.1016/j.applthermaleng.2016.08.120>
11. Kong J, Xu ZS, You WJ, Wang BL, Liang Y, Chen T (2021) Study of smoke back-layering length with different longitudinal fire locations in inclined tunnels under natural ventilation. *Tunn Undergr Space Technol* 107:103663. <https://doi.org/10.1016/j.tust.2020.103663>
12. Cano-Moreno JD, Pedro D, Esteban JMMS, Esteban BS et al (2021) Influence of the slope and delay on passenger evacuation from a fire along a railway tunnel with natural ventilation. *Fire Technol* 57:1569–1588. <https://doi.org/10.1007/s10694-020-01067-w>
13. Bullen ML (1977) Effect of a sprinkler on the stability of a smoke layer beneath a ceiling. *Fire Technol* 13(1):21–34

14. Bu RW, Yang HY, Xie Y, Zhao WQ, Fan CG, Guo ZW, Zhou Y (2022) Application of the high-pressure water mist system in a railway tunnel rescue station. *Therm Sci Eng Progr* 35:101467. <https://doi.org/10.1016/j.tsep.2022.101467>
15. Li QW, Zhang P, Guo S, Pan RM, Qin J, Liao GX (2013) Experimental study on suppression of n-heptane pool fire with water mist under longitudinal ventilation in long and narrow spaces. *Procedia Eng* 62:946–953. <https://doi.org/10.1016/j.proeng.2013.08.147>
16. Luan D, Bu RW, Sheng ZQ, Fan CG, Huang XY (2023) Experimental study on the impact of asymmetric heavy rainfall on the smoke spread and stratification dynamics in tunnel fires. *Tunn Undergr Space Technol* 134:104992. <https://doi.org/10.1016/j.tust.2023.104992>
17. Wang J, Wei YQ, Xie ZC, Jiang XP, Zhang HJ, Lu KH (2020) Influence of the water spray flow rate and angle on the critical velocity in tunnels with longitudinal ventilation. *Energy* 190:116466. <https://doi.org/10.1016/j.energy.2019.116466>
18. Deng T, Norris S, Sharma RN (2023) Stability of smoke stratification under the impact of water sprays with various droplet size ranges in longitudinally ventilated road tunnels. *Tunn Undergr Space Technol* 140:105262. <https://doi.org/10.1016/j.tust.2023.105262>
19. Wang ZY, Jiang XP, Wang QR, Wang BW (2022) Numerical investigation of water curtain for smoke blocking and heat insulation in urban underground road. *Therm Sci Eng Progr* 35:101468. <https://doi.org/10.1016/j.tsep.2022.101468>
20. Newman JS (1984) Experimental evaluation of fire-induced stratification. *Combust Flame* 57(1):33–39. [https://doi.org/10.1016/0010-2180\(84\)90135-4](https://doi.org/10.1016/0010-2180(84)90135-4)
21. Nyman H, Ingason H (2012) Temperature stratification in tunnels. *Fire Saf J* 48(2):30–37. <https://doi.org/10.1016/j.firesaf.2011.11.002>
22. Ingason H (2007) Correlation between temperatures and oxygen measurements in a tunnel flow. *Fire Saf J* 42(1):75–80. <https://doi.org/10.1016/j.firesaf.2006.08.003>
23. Huang DF, Li SC (2018) An experimental investigation of stratification characteristic of fire smoke in the corridor under the effect of outdoor wind. *J Wind Eng Ind Aerod* 179:173–183. <https://doi.org/10.1016/j.jweia.2018.05.021>
24. Tang F, Zhao Z, Zhao K (2020) Experimental investigation on carriage fires hazards in the longitudinally ventilated tunnels: assessment of the smoke stratification features. *Saf Sci* 130:104901. <https://doi.org/10.1016/j.ssci.2020.104901>
25. Li Z, Zhang Y, Jiang H et al (2022) Effect of fire source elevation on the smoke spreading characteristics in an extra-long tunnel. *Fire Technol* . <https://doi.org/10.1007/s10694-022-01299-y>
26. Jiang XP, Chen XG, Xiao NQ, Liao XJ, Fan CG (2021) Influence of the competitive effect of V-shaped slope tunnel on smoke characteristics. *Tunn Undergr Space Technol* 118:104193. <https://doi.org/10.1016/j.tust.2021.104193>
27. Xu HSH, Lu KH, Hu F, Ding YM, Li B (2024) Investigation on the restrain effect of air curtain to the spilled flame and its heat flux of a compartment-facade fire. *Appl Therm Eng* 256:124072. <https://doi.org/10.1016/j.applthermaleng.2024.124072>
28. Emmons HW (1991) The ceiling jet in fires. *Fire Saf Sci* 3:249–260
29. Willians C (1993) The downward movement of smoke due to a sprinkler spray. South Bank University, PhD
30. Li KY, Hu LH, Huo R, Li YZ et al (2009) A mathematical model on interaction of smoke layer with sprinkler spray. *Fire Saf J* 44:96–105
31. Tang Z, Vierendeels J, Fang Z, Merci B (2012) Description and application of an analytical model to quantify downward smoke displacement caused by a water spray. *Fire Saf J* 55:50–60. <https://doi.org/10.1016/j.firesaf.2012.10.012>

32. Wang J, Gao DM, Kong XW, Jiang XP, Lu KH (2023) Water spray effects on fire smoke temperature distribution beneath a symmetrical V-shaped tunnel ceiling. *Case Stud Therm Eng* 51:103568. <https://doi.org/10.1016/j.csite.2023.103568>
33. Janssens M, Tran H (1992) Data reduction of room tests for zone model validation. *J Fire Sci* 10(6):528–555
34. Lu H, Xu ZS, Markert F et al (2021) Study on the effect of tunnel dimensions on the smoke layer thickness in naturally ventilated short tunnel fires. *Tunn Undergr Space Technol* 112:103941. <https://doi.org/10.1016/j.tust.2021.103941>
35. Zhao SZ, Xu L, Obadi I, Wang F, Fang L, Weng MC (2020) Plug-holing height and complete plug-holing phenomenon in naturally ventilated tunnel fires with vertical shaft. *Tunn Undergr Space Technol* 107:103631. <https://doi.org/10.1016/j.tust.2020.103631>
36. Tanno A, Oka H, Kamiya K, Oka Y (2021) Determination of smoke layer thickness using vertical temperature distribution in tunnel fires under natural ventilation. *Tunn Undergr Space Technol* 119:104257. <https://doi.org/10.1016/j.tust.2021.104257>
37. McGrattan K, Hostikka S, Floyd JE (2016) Fire dynamics simulator, user's guide. NIST Spec Publ 1019:6
38. McGrattan K, Hostikka S, Floyd JE (2016) Fire dynamics simulator, technical reference guide. NIST Spec Publ 1018(1):1–206
39. Hurley MJ, Munguia A (2010) Analysis of prediction capability of FDS for response of thermal detectors. *J Fire Prot Eng* 20(2):77–99
40. Wang JH, Nie QM, Fang Z, Tang Z (2018) CFD simulations of the interaction of the water mist zone and tunnel fire smoke in reduced-scale experiments. *Procedia Eng* 211:726–735
41. Yan ZG, Guo QH, Zhu HH (2017) Full-scale experiments on fire characteristics of road tunnel at high altitude. *Tunn Undergr Space Technol* 66:134–146. <https://doi.org/10.1016/j.tust.2017.04.007>
42. Shafee S, Yozgatligil A (2018) An analysis of tunnel fire characteristics under the effects of vehicular blockage and tunnel inclination. *Tunn Undergr Space Technol* 79:274–285. <https://doi.org/10.1016/j.tust.2018.05.019>
43. Jia Y, Fan XL, Zhao XJ, Deng YL, Zhu XL, Zhao WF (2021) Study on the longitudinal ceiling temperature distribution induced by double pool fires in a tunnel. *Int J Therm Sci* 168:107059. <https://doi.org/10.1016/j.ijthermalsci.2021.107059>
44. Li YZ, Ingason H (2012) The maximum ceiling gas temperature in a large tunnel fire. *Fire Saf J* 48:38–48. <https://doi.org/10.1016/j.firesaf.2011.12.011>
45. Kunsch JP (1999) Critical velocity and range of a fire-gas plume in a ventilated tunnel. *J Atmos Environ* 33:13–24

Publisher's Note Springer Nature remains neutral with regard to jurisdictional claims in published maps and institutional affiliations.

Springer Nature or its licensor (e.g. a society or other partner) holds exclusive rights to this article under a publishing agreement with the author(s) or other rightsholder(s); author self-archiving of the accepted manuscript version of this article is solely governed by the terms of such publishing agreement and applicable law.